

# Comparing Reactivities of Metal Complexes in Solution and on Surfaces by IR Spectroscopy and Time-Resolved in Situ Ellipsometry

Thomas Vallant, Walter Simanko, Helmut Brunner, Ulrich Mayer,  
Helmuth Hoffmann,<sup>\*,†</sup> Roland Schmid, and Karl Kirchner<sup>\*,‡</sup>

*Institute of Inorganic Chemistry, Vienna University of Technology, Getreidemarkt 9,  
A-1060 Vienna, Austria*

Robert Svagera, Gerrit Schügerl, and Maria Ebel

*Institute of Applied and Technical Physics, Vienna University of Technology,  
Wiedner Hauptstrasse 8-10, A-1040 Vienna, Austria*

Received May 6, 1999

The reaction of the  $[\text{Ru}(\eta^5\text{-C}_5\text{H}_5)(\eta^4\text{-C}_5\text{H}_4\text{O})]^+$  fragment, anchored to self-assembled primer layers of  $\text{NC}_5\text{H}_4(\text{CH}_2)_2\text{SiO}_x$  or  $\text{NC}(\text{CH}_2)_{16}\text{SiO}_x$  on native silicon ( $\text{Si}/\text{SiO}_2$ ) substrates, with some tertiary phosphines  $\text{PR}_3$  has been studied by means of in situ ellipsometry. In this way the metal center is effectively inaccessible, and the phosphine can attack only at the cyclopentadienone ligand site. The rate constants derived from in situ ellipsometry are found to be in surprisingly good agreement with those obtained in homogeneous solution for the reaction of  $[\text{Ru}(\eta^5\text{-C}_5\text{H}_5)(\eta^4\text{-C}_5\text{H}_4\text{O})\text{L}]^+$  ( $\text{L} = \text{pyridine}, \text{CH}_3\text{CN}$ ) with  $\text{PR}_3$  to yield the  $\eta^3$ -cyclopentenoyl complexes  $[\text{Ru}(\eta^5\text{-C}_5\text{H}_5)(\eta^3\text{-C}_5\text{H}_4\text{O}-2\text{-PR}_3)\text{L}]^+$ . The nature of the ruthenium complexes at the surface has been established by IR spectroscopy in combination with XPS measurements. Thus, the present study provides a rare example of a direct comparison of the same intrinsic reaction occurring in homogeneous solution and at the solid–liquid interface.

## Introduction

Nucleophilic attack at metal-coordinated ligands is an important route in synthetic organic chemistry for obtaining regio- and stereoselectively new functionalized molecules.<sup>1</sup> Such a process is particularly facile when the metal center is coordinatively saturated, substitutionally inert, and sufficiently electron deficient, and when the ligand to be attacked is a conjugated or nonconjugated olefin.<sup>2</sup> Recently we have been investigating the nucleophilic attack of some tertiary phosphines at the cationic 18-electron complexes  $[\text{Ru}(\eta^5\text{-C}_5\text{H}_5)(\eta^4\text{-C}_5\text{H}_4\text{O})(\text{L})]^+$  ( $\text{L} = \text{CH}_3\text{CN}, \text{pyridine}$ ), finding two distinct targets of attack: the metal center, to give  $[\text{Ru}(\eta^3\text{-C}_5\text{H}_5)(\eta^4\text{-C}_5\text{H}_4\text{O})(\text{PR}_3)(\text{L})]^+$  (Figure 1, pathway 1), or the diene ligand, to give  $[\text{Ru}(\eta^5\text{-C}_5\text{H}_5)(\eta^3\text{-C}_5\text{H}_4\text{O}-\text{PR}_3)(\text{L})]^+$  (Figure 1, pathway 2).<sup>3,4</sup> Which mode is pursued appears to be guided by the basicity of the phosphine. Whereas weakly basic phosphines have no clear preference, with both ways followed simulta-

neously and competitively, strongly basic phosphines definitely prefer to attack the metal center. This latter course is also adopted by the very bulky  $\text{PCy}_3$  (cone angle  $\sim 170^\circ$ ), implying that the mode of attack is rather insensitive to steric conditions. To prevent strong nucleophiles from attacking the metal center, in other words, to control the regioselectivity, we attempted to immobilize the metal center in a monolayer film of  $[\text{Ru}(\eta^5\text{-C}_5\text{H}_5)(\eta^4\text{-C}_5\text{H}_4\text{O})]^+$  fragments anchored to self-assembled primer layers ( $\text{L} = \text{NC}_5\text{H}_4(\text{CH}_2)_2\text{SiO}_x$  or  $\text{NC}(\text{CH}_2)_{16}\text{SiO}_x$ ) on native silicon ( $\text{Si}/\text{SiO}_2$ ) substrates. The rigid geometry and high packing density of the film molecules achievable in such highly organized monolayers have previously been shown to alter the solution-phase reactivities dramatically, leaving only the surface-exposed groups accessible to reaction.<sup>5</sup> In our case, the coordination of the ruthenium atoms to the terminal nitrogens of the primer layer was expected to bury the metal centers underneath a blanket of diene ligands, thereby forcing the reaction with nucleophiles onto pathway 2' (Figure 1). To test this hypothesis, we exposed the surface-confined metal complex to solutions of various tertiary phosphines  $\text{PR}_3$  ( $\text{P}(n\text{-octyl})_3$ ,  $\text{P}(n\text{-Bu})_3$ ,  $\text{PPhMe}_2$ ,  $\text{PPh}_2\text{Me}$ ,  $\text{tris}(2,4,6\text{-trimethoxyphenyl})\text{phosphine}$  (TTP)) and monitored the thickness increase of the adsorbate film by means of in situ ellipsometry. As we have shown recently,<sup>6</sup> this method provides direct

<sup>†</sup> E-mail: hhoffman@email.tuwien.ac.at.

<sup>‡</sup> E-mail: kkirch@mail.zserv.tuwien.ac.at.

(1) Collman, J. P.; Hegedus, L. S.; Norton, J. R.; Finke, R. G. *Principles and Applications of Organotransition Chemistry*, 2nd ed.; University Science Books: Mill Valley, CA, 1987.

(2) Davies, S. G.; Green, M. L. H.; Mingos, D. M. P. *Tetrahedron* **1978**, *34*, 3047.

(3) (a) Simanko, W.; Sapunov, V. N.; Schmid, R.; Kirchner, K.; Wherland, S. *Organometallics* **1998**, *17*, 2391. (b) Simanko, W.; Sapunov, V. N.; Schmid, R.; Kirchner, K.; Coddington, J.; Wherland, S. *Organometallics* **1998**, *17*, 5674.

(4) Simanko, W.; Vallant, T.; Mereiter, K.; Schmid, R.; Kirchner, K.; Coddington, J.; Wherland, S. *Inorg. Chem.* **1996**, *35*, 5923.

(5) Maoz, R.; Sagiv, J. *Langmuir* **1987**, *3*, 1045.

(6) Brunner, H.; Vallant, T.; Mayer, U.; Hoffmann, H. *J. Colloid Interface Sci.* **1999**, *212*, 545.

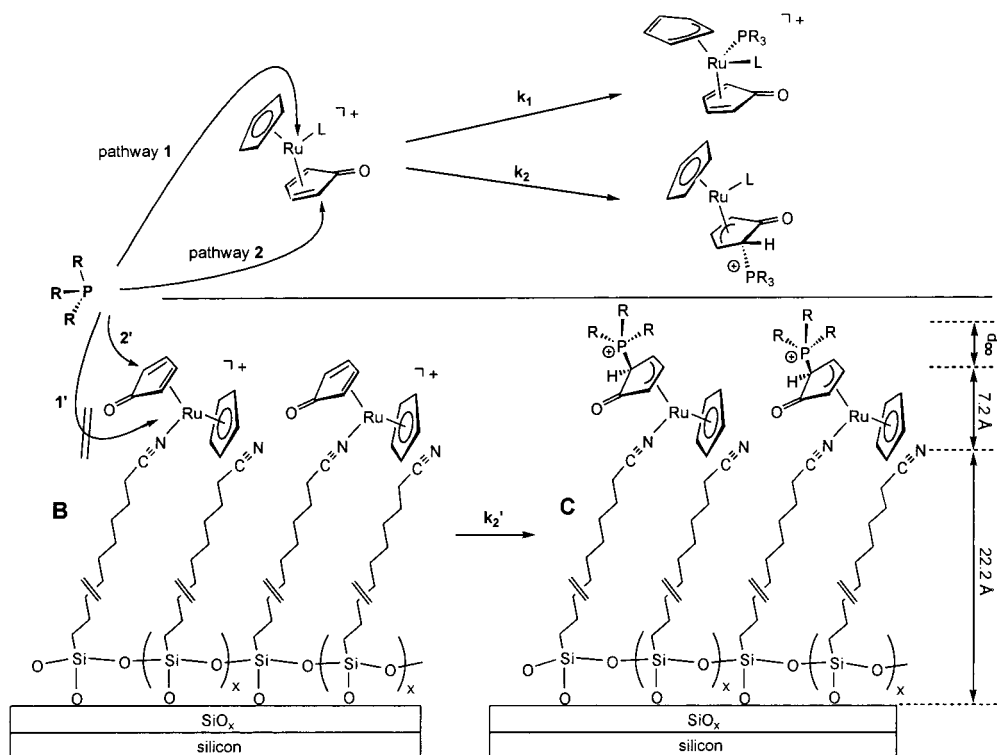


**Figure 1.** Nucleophilic attack of PR<sub>3</sub> at the [Ru(η<sup>5</sup>-C<sub>5</sub>H<sub>5</sub>)(η<sup>4</sup>-C<sub>5</sub>H<sub>4</sub>O)]<sup>+</sup> fragment in solution (upper part) and at the surface (lower part).

kinetic information about reactions at the solid/liquid interface in the monolayer and submonolayer regime. In addition, we have used IR spectroscopy to probe the course of the surface reactions and to obtain information about the surface orientation of the adsorbate molecules.

### Experimental Section

**General Information.** Manipulations were performed under an inert atmosphere of nitrogen by using standard Schlenk techniques and/or a glovebox. All chemicals were standard reagent grade and were used without further purification. The solvents were purified according to standard procedures.<sup>7</sup> [Ru(η<sup>5</sup>-C<sub>5</sub>H<sub>5</sub>)(η<sup>4</sup>-C<sub>5</sub>H<sub>4</sub>O)]<sub>2</sub>(CF<sub>3</sub>SO<sub>3</sub>)<sub>2</sub> (1) was prepared according to the literature using AgCF<sub>3</sub>SO<sub>3</sub> instead of AgPF<sub>6</sub>.<sup>8</sup> P-doped, (100) oriented, and single-sided polished silicon wafers (Wacker Chemitronic, test grade, 14–30 Ω cm resistivity, 0.5 mm thickness) were cut into pieces of appropriate size (25 × 15 mm<sup>2</sup>) and were cleaned by treating with ultrasound in toluene, rinsing with acetone and ethanol, and blow-drying in high-purity nitrogen, followed by a 15 min exposure to an UV/ozone atmosphere in a commercial cleaning chamber (Boeckel Industries, Model UVclean) equipped with a low-pressure mercury quartz lamp (λ<sub>max</sub> = 185 and 254 nm). This treatment yields a hydrophilic, contamination-free surface with a native oxide layer of 12–14 Å thickness, as routinely checked by ellipsometry. Powdered silica (Aldrich, 99.99%) was exposed to an UV/ozone atmosphere for 10 min prior to the adsorption experiments. Transmission infrared spectra were recorded with a Mattson RS FT-IR spectrometer. For the external reflection infrared spectra a custom-made reflection optical system was connected to the spectrometer, as described in detail elsewhere.<sup>9</sup> p-Polarized light at 80° incidence was used. For transmission FT-IR spectra powdered silica was

pressed into KBr pellets with a concentration of 5 wt %. A total of 1024 scans for external reflection and 256 scans for transmission spectra at 4 cm<sup>-1</sup> resolution were averaged from the sample and the reference. <sup>1</sup>H and <sup>31</sup>P{<sup>1</sup>H} NMR spectra were recorded on a Bruker AC-250 spectrometer operating at 250.13 and 101.26 MHz, respectively, and were referenced to SiMe<sub>4</sub> and H<sub>3</sub>PO<sub>4</sub> (85%).

**Ellipsometry.** The ellipsometric measurements were carried out on a Plasmos SD 2300 ellipsometer with a rotating analyzer and a He–Ne laser (λ = 632.8 nm) as the light source. The experimental procedures and data analysis are described in detail in ref 6. Briefly, ex situ measurements were performed in air as the ambient medium at an incidence angle of 68°. A four-phase model (Si/SiO<sub>2</sub>/adsorbate/air) was used to determine the thickness of an adsorbate layer, which required the previous determination of the SiO<sub>2</sub> thickness of the clean substrate. The error margins were determined by averaging the results of two to four individual samples and three different spots on each sample surface. In situ experiments of phosphine adsorption onto the surface-confined metal complexes were carried out in a home-built glass cell at 68° incidence with the adsorbate solution in direct contact with the substrate. The primed substrate was mounted and aligned in the cell, which was subsequently filled with pure solvent. Start values of the ellipsometric angles Φ and Δ (amplitude ratio and phase shift, respectively, between s- and p-polarized components of the probing laser radiation) were determined, a calculated volume of phosphine reagent, corresponding to the desired concentration, was injected, and Φ and Δ were monitored as a function of time. After completion of the surface reaction, indicated by constant Φ and Δ values, the sample was removed from the cell and the thickness of the adsorbed phosphine layer was measured in air to verify a complete and homogeneous monolayer deposition.

**XPS Measurements.** Native silicon substrates covered with different sample layers were analyzed with a Kratos XSAM 800 spectrometer using a twin anode (Mg, Al) X-ray tube without monochromator as excitation source. The acquired photoelectron spectra were excited by Mg Kα<sub>1,2</sub> radi-

(7) Perrin, D. D.; Armarego, W. L. F. *Purification of Laboratory Chemicals*, 3rd ed.; Pergamon: New York, 1988.

(8) Kirchner, K.; Taube, H. *J. Am. Chem. Soc.* **1991**, *113*, 7039.

(9) Hoffmann, H.; Mayer, U.; Brunner, B.; Krischanitz, A. *Vib. Spectrosc.* **1995**, *8*, 151.

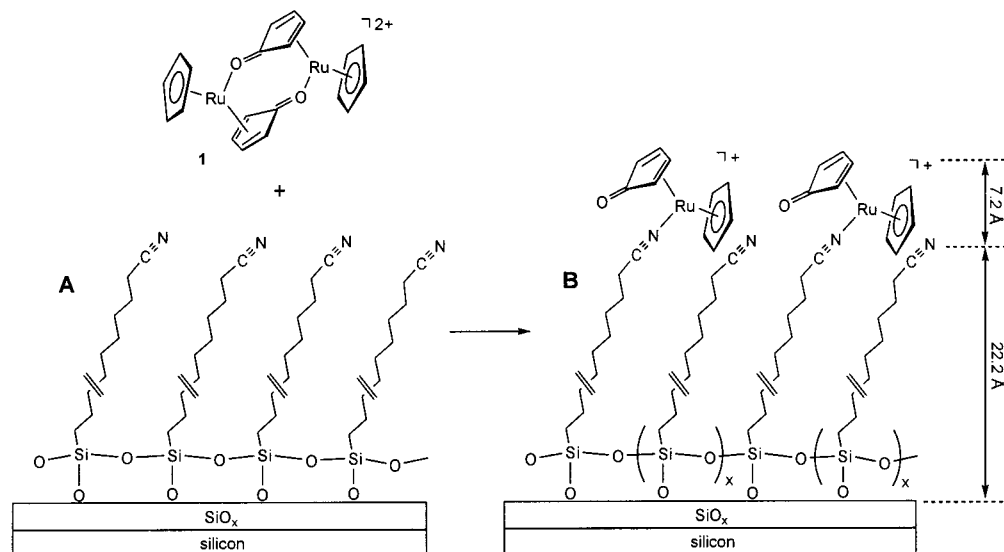


**Figure 2.** Reaction of  $[\text{Ru}(\eta^5\text{-C}_5\text{H}_5)(\eta^4\text{-C}_5\text{H}_4\text{O})]_2(\text{CF}_3\text{SO}_3)_2$  (**1**) with a primer monolayer of  $\text{SiO}_x(\text{CH}_2)_{16}\text{CN}$  adsorbed on a native silicon substrate (**A**).

tion and by the satellite lines  $\text{Mg K}\alpha_{3,4}$ . The angle between the X-rays and the detected electrons was fixed to  $70^\circ$ , and the samples were aligned in a way that the analyzer was located along the normal to the sample surface. The following photoelectron peaks were evaluated for each sample: C1s, N1s, O1s, F1s, Si2p, and Ru3p<sub>3/2</sub>. Prior to integration a Shirley background was subtracted. Ratios between atom concentrations of the elements N, Ru, and F were calculated by a quantitative XPS analysis algorithm<sup>10</sup> based on fundamental parameters taking into account the layered structure of specimens.

## Results and Discussion

Monolayers of  $\text{SiO}_x(\text{CH}_2)_2\text{C}_5\text{H}_4\text{N}$  and  $\text{SiO}_x(\text{CH}_2)_{16}\text{CN}$  were formed on native silicon substrates via self-assembling<sup>11</sup> by immersing the clean substrates into 1 mM solutions of  $\text{SiCl}_3(\text{CH}_2)_2\text{C}_5\text{H}_4\text{N}$  and  $\text{SiCl}_3(\text{CH}_2)_{16}\text{CN}$ , respectively, in *n*-hexane for 2 h. Film thicknesses of 9.8 and 23.2 Å, respectively, were measured ellipsometrically for these primer layers. The  $[\text{Ru}(\eta^5\text{-C}_5\text{H}_5)(\eta^4\text{-C}_5\text{H}_4\text{O})]^+$  moiety was then attached to the nitrogen-terminated surface by overnight immersion of the primed substrates in a solution of the dimeric complex **1** (2 mM) in nitromethane (Figure 2). A thickness increase of 7.2 Å, in close agreement with the size of the  $[\text{Ru}(\eta^5\text{-C}_5\text{H}_5)(\eta^4\text{-C}_5\text{H}_4\text{O})]^+$  fragment estimated from X-ray diffraction data,<sup>12</sup> was measured after this treatment and indicated a monolayer deposition of the metal complex. This bilayer film was then transferred to an in situ liquid cell, which subsequently was filled with the phosphine solution in acetone, resulting in a large excess of the phosphine over the surface-bound metal complex (pseudo-first-order conditions). The surface reaction between the two components was monitored by the measured changes of the ellipsometric angles  $\Psi$  and  $\Delta$ , which were converted into average film thicknesses  $d_t$  and surface coverages  $\Theta_t = d_t/d_\infty$  ( $d_\infty$  = final thickness

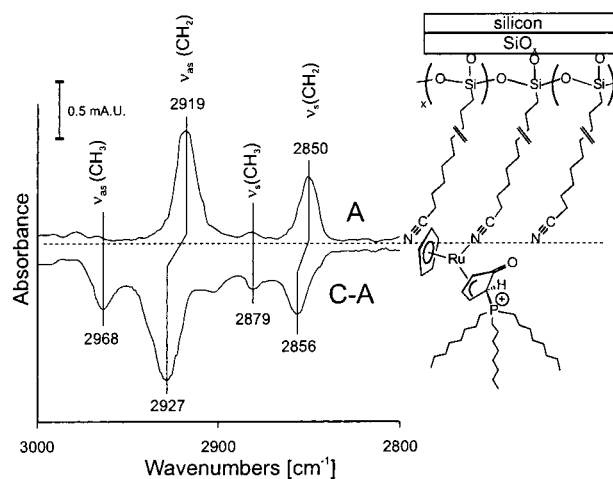


**Figure 3.** External reflection infrared spectra of a  $\text{SiO}_x(\text{CH}_2)_{16}\text{CN}$  primer layer adsorbed on a native silicon substrate (**A**) and of the  $\text{P}(n\text{-octyl})_3$  phosphine overlayer (**C-A**) in a film of  $[\text{Ru}(\eta^5\text{-C}_5\text{H}_5)(\eta^3\text{-C}_5\text{H}_4\text{O}-2\text{-P}(n\text{-octyl})_3)(\text{NC}(\text{CH}_2)_{16}\text{SiO}_x)]^+$ .

for the complete monolayer film), as described in detail elsewhere.<sup>6</sup> The formation of a phosphine monolayer in the course of this reaction could also be detected in the case of  $\text{P}(n\text{-octyl})_3$  and  $\text{P}(n\text{-Bu})_3$  by the growth of  $\text{CH}_2$  stretching absorptions in the IR reflection spectra, as shown in Figure 3. The peak frequencies and intensities of the  $\text{CH}_2$  stretching vibrations, which have been shown to be a sensitive probe for the average film structure, in particular on nonmetal substrates,<sup>13</sup> indicate a fairly disordered orientation and loose packing of the alkyl substituents in the terminal phosphine layer. This is evidenced in the bottom spectrum of Figure 3 by inverted, downward-pointing  $\text{CH}$  stretching absorptions ( $\nu_a(\text{CH}_2)$  at  $2927\text{ cm}^{-1}$  and  $\nu_s(\text{CH}_2)$  at  $2855\text{ cm}^{-1}$ ), implying tilt angles of the corresponding vibrational dipoles close to the isotropic, "magic" angle of  $55^\circ$  with respect to the surface normal.<sup>14</sup> The spectrum of the

(10) Hanke, W.; Ebel, H.; Ebel, M. F.; Jablonski, A.; Hirokawa, K. *J. Electron Spectrosc. Relat. Phenom.* **1986**, *40*, 241.

(11) Ulman, A. *Chem. Rev.* **1996**, *96*, 1533.

(12) (a) Kirchner, K.; Taube, H.; Scott, B.; Willett, R. D. *Inorg. Chem.* **1993**, *32*, 1430. (b) Kirchner, K.; Schmid, R.; Mereiter, K. *Acta Crystallogr.* **1995**, *C51*, 361. (c) Smith, T. P.; Kwan, K. S.; Taube, H.; Bino, A.; Cohen, S. *Inorg. Chem.* **1984**, *23*, 1943.

(13) Hoffmann, H.; Mayer, U.; Krischanitz, A. *Langmuir* **1995**, *11*, 1304.

(14) Vallant, T.; Brunner, H.; Mayer, U.; Hoffmann, H. *Langmuir* **1998**, *14*, 5826.

**Table 1. Second-Order Rate Constants from in Situ Ellipsometric and Stopped-Flow Spectrophotometric Measurements for the Reaction of  $[\text{Ru}(\eta^5\text{-C}_5\text{H}_5)(\eta^4\text{-C}_5\text{H}_4\text{O})(\text{L})](\text{CF}_3\text{SO}_3)$  with  $\text{PR}_3$  in Acetone at 20 °C**

PR <sub>3</sub>	L = SiO <sub>x</sub> (CH <sub>2</sub> ) <sub>2</sub> C <sub>5</sub> H <sub>4</sub> N or C <sub>5</sub> H <sub>5</sub> N				L = SiO <sub>x</sub> (CH <sub>2</sub> ) <sub>16</sub> CN or CH <sub>3</sub> CN			
	$k_2'$ , M <sup>-1</sup> s <sup>-1</sup> <sup>a</sup>	$k_2$ , M <sup>-1</sup> s <sup>-1</sup> <sup>b</sup>	$k_1$ , M <sup>-1</sup> s <sup>-1</sup> <sup>b</sup>	$d_{\infty}$ , Å <sup>c</sup>	$k_2'$ , M <sup>-1</sup> s <sup>-1</sup> <sup>a</sup>	$k_2$ , M <sup>-1</sup> s <sup>-1</sup> <sup>b</sup>	$k_1$ , M <sup>-1</sup> s <sup>-1</sup> <sup>b</sup>	$d_{\infty}$ , Å <sup>c</sup>
P( <i>n</i> -octyl) <sub>3</sub>	0.17 ± 0.05			13.5	0.87 ± 0.09			13.7
P( <i>n</i> -Bu) <sub>3</sub>	0.23 ± 0.1	0.22 ± 0.01	149 ± 13	7.1	0.94 ± 0.2	<i>e</i>	756 ± 38	7.2
PPhMe <sub>2</sub>	0.21 ± 0.03	0.17 ± 0.01	206 ± 15	4.5	1.3 ± 0.3	<i>e</i>	484 ± 24	4.7
PPh <sub>2</sub> Me	0.014 ± 0.004	0.050 ± 0.001	<i>e</i>	5.3	2.0 ± 0.2	1.4 ± 0.05	418 ± 34	5.5
TTP <sup>d</sup>	43 ± 2	38 ± 2	<i>e</i>	8.2	229 ± 6	1241 ± 40	<i>e</i>	8.1

<sup>a</sup> In situ ellipsometry. <sup>b</sup> Stopped-flow spectrophotometry. <sup>c</sup>  $d_{\infty}$  = increase in the film thicknesses (standard deviation ±1). <sup>d</sup> TTP = tris(2,4,6-trimethoxyphenyl)phosphine. <sup>e</sup> Not observable in solution.<sup>3</sup>

SiO<sub>x</sub>(CH<sub>2</sub>)<sub>16</sub>CN primer layer (Figure 3A), on the other hand, shows regular upward-pointing  $\nu(\text{CH})$  absorptions at lower frequencies ( $\nu_{\text{as}}(\text{CH}_2)$  at 2919 cm<sup>-1</sup> and  $\nu_{\text{s}}(\text{CH}_2)$  at 2850 cm<sup>-1</sup>), which are characteristic of a densely packed, highly ordered film structure with close-to-perpendicular orientation of the hydrocarbon chains on the substrate surface.<sup>12,13</sup> No changes are observed for the  $\nu(\text{CH}_2)$  absorptions after coordination of the Ru complex. Several factors are believed to cause the structural differences between the siloxane primer layer and the phosphine overlayer: First, van der Waals interactions between the hydrocarbon chains, which are the driving force for a uniform crystalline-like packing of the film molecules, are significantly reduced in the short-chain (C8) phosphine layer compared to the long-chain (C16) siloxane layer. Second, the surface density of coordination sites composed of the fairly large diene ligands is presumably incompatible with a densely packed arrangement of the smaller phosphine molecules, leaving sufficient empty space for the hydrocarbon chains in the overlayer to adopt random orientations. And third, as we have shown recently,<sup>15</sup> structural disorder progresses with increasing layer number even in multilayers with identical compositions and sizes of the film molecules.

The surface coverage  $\Theta_t$  of the phosphine ligand as a function of time was analyzed by means of a simple Langmuir model for an irreversible adsorption process, where  $\Theta_t = 1 - \exp[-k_2'ct]$  ( $k_2'$  = second-order adsorption rate constant,  $c$  = phosphine concentration,  $t$  = adsorption time). The rate constants  $k_2'$  were determined from the logarithmic plots of  $\ln(1 - \Theta_t)$  vs  $t$  for different phosphine concentrations, as shown in Figure 4 for TTP as the nucleophilic reactant. These are compared in Table 1 to the rate constants  $k_1$  (attack at the metal center) and  $k_2$  (attack at the diene ligand) for the solution-phase reactions determined by stopped-flow spectrophotometry. A surprisingly good agreement between the  $k_2$  (solution) and  $k_2'$  (surface) rate constants over more than 3 orders of magnitude is found. For the reaction at the surface with L = SiO<sub>x</sub>(CH<sub>2</sub>)<sub>2</sub>C<sub>5</sub>H<sub>4</sub>N and the tertiary phosphines P(*n*-Bu)<sub>3</sub>, PPhMe<sub>2</sub>, PPh<sub>2</sub>Me, and TTP the apparent rate constants  $k_2'$  are 0.23, 0.21, 0.014, and 43 M<sup>-1</sup> s<sup>-1</sup>, respectively, while for the analogous reactions in solution rate constants  $k_2$  of 0.22, 0.17, 0.050, and 38 M<sup>-1</sup> s<sup>-1</sup> have been determined. These findings strongly suggest that the metal center is effectively inaccessible in the surface-confined state and that the phosphine can attack only at the cyclopentadienone ligand site, as outlined in Figure 1.

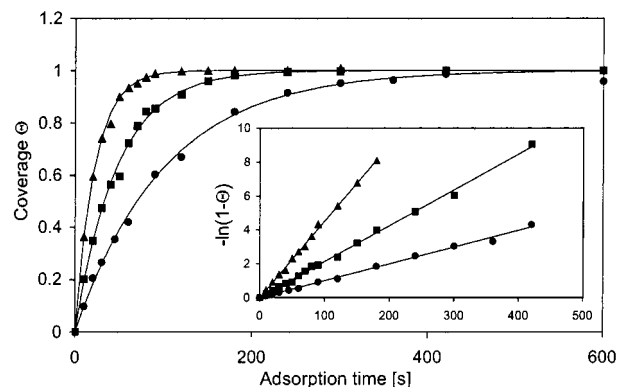


**Figure 4.** Surface coverage  $\Theta$  as a function of time derived from in situ ellipsometric measurements for the reaction of TTP (▲, 1 mM; ■, 0.5 mM; ●, 0.25 mM) in acetone with  $[\text{Ru}(\eta^5\text{-C}_5\text{H}_5)(\eta^4\text{-C}_5\text{H}_4\text{O})(\text{NC}(\text{CH}_2)_{16}\text{SiO}_x)]^+$  anchored to a silicon surface (B).

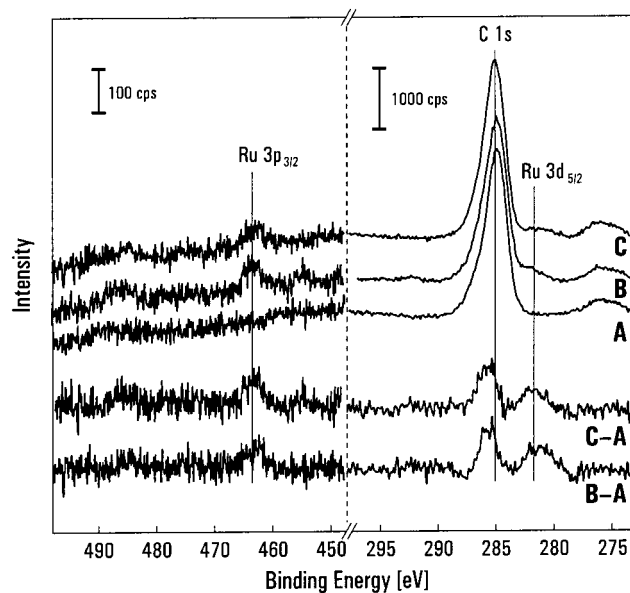


**Figure 5.** Photoelectron spectra of a SiO<sub>x</sub>(CH<sub>2</sub>)<sub>16</sub>CN primer layer adsorbed on a native silicon substrate (A), of  $[\text{Ru}(\eta^5\text{-C}_5\text{H}_5)(\eta^4\text{-C}_5\text{H}_4\text{O})(\text{NC}(\text{CH}_2)_{16}\text{SiO}_x)]^+$  (B), and of  $[\text{Ru}(\eta^5\text{-C}_5\text{H}_5)(\eta^3\text{-C}_5\text{H}_4\text{O}-2\text{-P}(\textit{n}\text{-Bu})_3)(\text{NC}(\text{CH}_2)_{16}\text{SiO}_x)]^+$  (C) in the binding energy range of Ru 3p<sub>3/2</sub> and Ru 3d<sub>5/2</sub>. In the difference spectra, shown in the lower part, the C 1s signal of the primer layer has been subtracted.

To obtain information about the oxidation states of the Ru center as well as the degree of heteroatomic coverage, XPS measurements have been undertaken (Figure 5). Unfortunately, the peak intensities of ruthenium in comparison to carbon are very small. Moreover, the characteristic Ru 3d<sub>5/2</sub> signal is situated

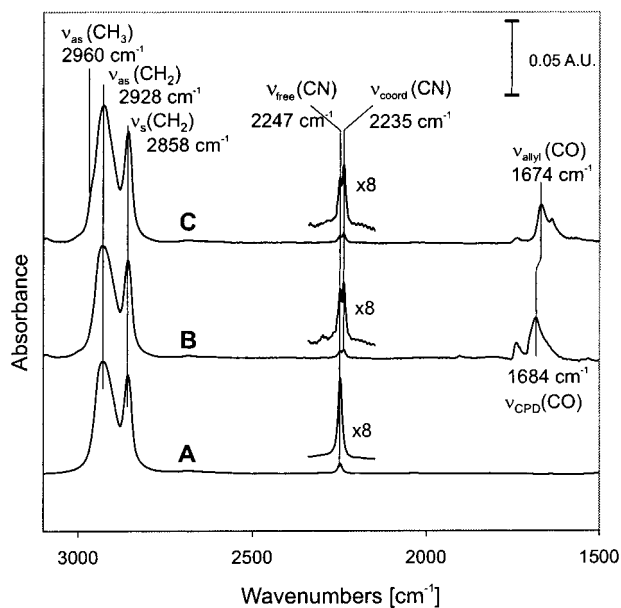


**Figure 6.** IR transmission spectra of (A)  $\text{SiO}_x(\text{CH}_2)_{16}\text{CN}$  adsorbed onto powdered silica, (B)  $[\text{Ru}(\eta^5\text{-C}_5\text{H}_5)(\eta^4\text{-C}_5\text{H}_4\text{O})]^+$  adsorbed onto A, and (C)  $\text{P}(n\text{-Bu})_3$  adsorbed onto B. The adsorbed silica samples were pressed into KBr pellets, and their IR spectra were referenced against clean  $\text{SiO}_2/\text{KBr}$  pellets with the same  $\text{SiO}_2$  concentration (5% w/w).

between the strong C 1s peak (arising from Mg  $\text{K}\alpha_{1,2}$ ) and the corresponding satellite (Mg  $\text{K}\alpha_{3,4}$ ). The Ru 3p<sub>3/2</sub> signal is also detectable but is very weak. Thus, the analytical significance of these XPS data and the chemical shift information contained therein are rather limited. An estimation of the atomic ratios Ru:N and Ru:F<sub>3</sub>, which were derived from model calculations based on a previously described algorithm,<sup>10</sup> yields values of 1:(10 ± 2) for Ru:N and 1:(1.5 ± 0.2) for Ru:F<sub>3</sub>, respectively. Whereas the Ru:N ratio gives at least the semiquantitative information that, on average, only 1 out of 10 CN groups are attached to a Ru complex, the N:F<sub>3</sub> ratio is clearly different from the expected value of 1:1, which derives from a simple charge balance between the metal complex cations and the  $\text{CF}_3\text{SO}_3^-$  counterions. This latter discrepancy may be caused by slow sample decomposition upon exposure to X-ray radiation in the XPS spectrometer.

Additional evidence for the proposed reaction route on the surface should be available from IR spectroscopic data of the  $\nu(\text{CO})$  and  $\nu(\text{CN})$  stretching vibrations of the adsorbed ruthenium complex. Unfortunately, these absorptions turned out to be too weak to be observed with the external reflection IR method on a plane silicon wafer. We have therefore carried out analogous experiments with powdered silica as the substrate and have measured the IR spectra of the adsorbate layers as conventional transmission spectra, which are depicted in Figure 6. Several previous studies have shown that the chemistry and structure of organosilane monolayers prepared by self-assembly on both powdered silica and plane native silicon wafers are very similar.<sup>16</sup> The spectrum of A in Figure 6 shows a  $\text{SiO}_x(\text{CH}_2)_{16}\text{CN}$

primer layer adsorbed on silica. The  $\nu(\text{CH}_2)$  stretching vibrations appear as strong absorptions at 2928 and 2858  $\text{cm}^{-1}$ . Their high-frequency shift compared to the primer layer spectrum on a flat silicon substrate (A in Figure 3) indicates a more disordered configuration and looser packing of the film molecules on the powdered substrates.<sup>16</sup> In addition, a distinct symmetric peak appears at 2247  $\text{cm}^{-1}$ , which is assigned to  $\nu(\text{CN})$ . Upon adsorption of the ruthenium complex  $[\text{Ru}(\eta^5\text{-C}_5\text{H}_5)(\eta^4\text{-C}_5\text{H}_4\text{O})]^+$ , this  $\nu(\text{CN})$  band is split into two components of about equal intensities and peak wavenumbers of 2247 and 2235  $\text{cm}^{-1}$  (B in Figure 6), whereas the  $\nu(\text{CH}_2)$  absorptions remain unchanged. Thus, the nitrile ligands bound to the ruthenium metal center give rise to a low-frequency shift ( $\pi$ -back-bonding is not a prominent feature in these complexes),<sup>12a</sup> and the  $\nu(\text{CN})$  frequency of the noncoordinated nitrogen sites remains unaffected. As opposed to the quantitative reaction of a nitrile with 1 in solution, this partial occupation of the CN sites on the surface can be explained both by the relatively large size of the ruthenium species, which sterically block adjacent CN ligands, and by the rather disordered orientation of the  $\text{SiO}_x(\text{CH}_2)_{16}\text{CN}$  molecules on a powdered silica substrate, by which some of the terminal CN groups may get buried in the hydrocarbon layer and become inaccessible for further reaction. On the flat silicon substrates, the percentage of coordinated CN sites appears to be even lower (ca. 10% according to XPS data), as a consequence of their increased packing density and/or their possibly reduced reactivity in this rigid, solidlike environment. The spectrum of B in Figure 6 shows, in addition to the  $\nu(\text{CN})$  absorption, the characteristic CO stretching vibration of the ruthenium cyclopentadienone (CPD) species<sup>12a</sup> at 1684  $\text{cm}^{-1}$ . Subsequent attack of the phosphine yields an  $\eta^3$ -cyclopentenoyl complex (C in Figure 6) with increased relative intensities of the  $\nu(\text{CH}_2)$  absorptions and a shoulder at 2960  $\text{cm}^{-1}$  from the terminal octyl groups. Both the  $\nu(\text{CN})$  and the  $\nu(\text{CO})$  absorptions, however, remain essentially unchanged,<sup>4</sup> which strongly supports the proposed reaction of the phosphine with the diene ligand. Nucleophilic attack at the metal center, in contrast, should result in a further low-frequency shift of  $\nu(\text{CN})$  and a  $\nu(\text{CO})$  peak appearing around 1580  $\text{cm}^{-1}$ , as shown recently.<sup>4</sup> Further evidence for this pathway comes from the fact that the immobilized  $\eta^3$ -cyclopentenoyl complex can be liberated on treatment with acid (0.5 M  $\text{CF}_3\text{SO}_3\text{H}$  in  $\text{CH}_3\text{NO}_2$ ) to give a 1,2-disubstituted ruthenocene.<sup>17</sup> This has been demonstrated with the  $\text{P}(n\text{-Bu})_3$  derivative, affording  $[\text{Ru}(\eta^5\text{-C}_5\text{H}_5)(\eta^5\text{-C}_5\text{H}_3\text{OH-2-PBu}^n_3)]^+$  (2) (Figure 7), as determined by  $^1\text{H}$  and  $^{31}\text{P}\{^1\text{H}\}$  NMR spectroscopy and comparison with an authentic sample.<sup>4</sup> The IR spectrum of the silica powder after treatment with acid was identical with that of A shown in Figure 6.

In summary, the present study provides a rare example of a direct comparison of the same intrinsic reaction occurring in homogeneous solution and at the solid-liquid interface. Along these lines, time-resolved in situ ellipsometry is introduced as a new tool for mechanistic studies of organometallic reactions, allowing the assessment of kinetic data that may be inac-

(16) (a) Brandriss, S.; Margel, S. *Langmuir* **1993**, *9*, 1232. (b) Tripp, C. P.; Hair, M. L. *Langmuir* **1992**, *8*, 1120. (c) Kallury, K. M. R.; MacDonald, P. M.; Thompson, M. *Langmuir* **1994**, *10*, 492.

(17) Vallant, T. Masters Thesis, Vienna University of Technology, Vienna, Austria, 1995.

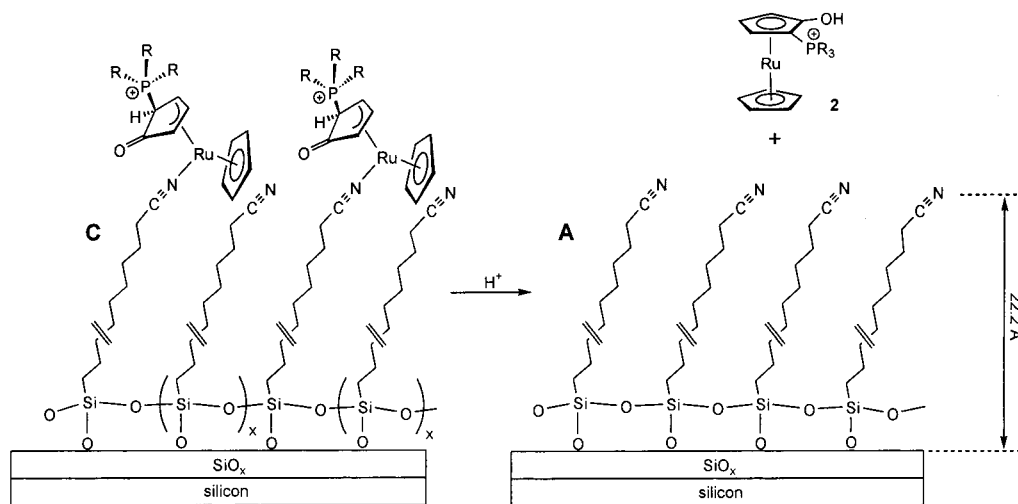


**Figure 7.** Reaction of  $\text{CF}_3\text{SO}_3\text{H}$  with  $[\text{Ru}(\eta^5\text{-C}_5\text{H}_5)(\eta^3\text{-C}_5\text{H}_4\text{O}-2\text{-P}(n\text{-Bu})_3)(\text{NC}(\text{CH}_2)_{16}\text{SiO}_x)]^+$  (**C**) adsorbed on silica powder.

cessible otherwise. The attack at the cyclopentadienone ligand in solution is several orders of magnitude slower than the attack at the metal center ( $k_2 \ll k_1$ ). Thus, the rate constants  $k_2$  are sometimes not directly determinable by stopped-flow measurements, in which case the surface immobilization of the metal complex gives an alternative access to these data.

**Acknowledgment.** Financial support by the "Fonds zur Förderung der wissenschaftlichen Forschung" (Project No. 9749) and the "Jubiläumsfonds der Österreichischen Nationalbank" (Project No. 6474) is gratefully acknowledged.

OM990340X